

cover the uncertainty in the calibration of the proton beam polarization. Their data shown for 119° (lab) were obtained by interpolation of measurements at 117.5° and 120° . In Figs. 2 and 3 the comparison is made for the same "compound-nuclear" energies by using two energy scales for E_n and E_p that are connected by the relation $E_n = E_p - 1.1$ MeV. Clearly the measured values of $A_y(\theta)$ for these two charge-symmetric reactions are identical within the accuracy of the experimental values. This is the first time $n + {}^4\text{He}$ data have been compared to the data of Bacher *et al.* for $p + {}^4\text{He}$ and the first illustration of the equality of $A_y(\theta)$ for $n + {}^4\text{He}$ and $p + {}^4\text{He}$ when they are compared in this way.

In summary, the reaction ${}^3\text{H}(d, n){}^4\text{He}$ can now be used to provide neutron beams from 20 to 30 MeV with a polarization known to about $\pm 2\%$. Such neutron beams were used to determine the ${}^4\text{He}(n, n){}^4\text{He}$ analyzing power $A_y(\theta)$ at 119° (lab) which is near the back-angle maximum. The data show that the phase shifts of Hoop and Barschall predict $A_y(119^\circ)$ fairly well above 22 MeV, but not in the immediate region below the 22-MeV resonance. The angular distribution data at 20.9 MeV favor the phase-shift sets of Lisowski and Walter⁹ and of Stammbach and Walter¹⁰ over earlier sets. Comparison to ${}^4\text{He}(p, p){}^4\text{He}$ experimental data at the same "compound-nuclear" energies shows that the results for the two charge-sym-

metric reactions are identical within the accuracy of the measurements.

*Work supported by the U. S. Energy Research and Development Administration.

†Visiting staff member at Los Alamos Scientific Laboratory, Los Alamos, N. Mex. 87545.

¹G. G. Ohlsen, P. W. Keaton, and J. L. Gammel, in Proceedings of the Third International Symposium on Polarization Phenomena in Nuclear Reactions, Madison, Wisconsin, 1970, edited by H. H. Barschall and W. Haerberli (Univ. of Wisconsin Press, Madison, Wis., 1971), p. 512.

²G. G. Ohlsen, Rep. Prog. Phys. **35**, 717 (1972).

³J. E. Simmons, W. B. Broste, T. R. Donoghue, R. C. Haight, and J. C. Martin, Nucl. Instrum. Methods **106**, 477 (1972).

⁴G. P. Lawrence, G. G. Ohlsen, and J. L. McKibben, Phys. Lett. **28B**, 594 (1969).

⁵G. G. Ohlsen, R. A. Hardekopf, P. W. Lisowski, and R. L. Walter, to be published.

⁶W. B. Broste, G. S. Mutchler, J. E. Simmons, R. A. Arndt, and L. D. Roper, Phys. Rev. C **5**, 761 (1972).

⁷G. S. Mutchler, W. B. Broste, and J. E. Simmons, Phys. Rev. C **3**, 1031 (1971).

⁸A. D. Bacher, G. R. Plattner, H. E. Conzett, D. J. Clark, H. Grunder, and W. F. Tivol, Phys. Rev. C **5**,

⁹P. W. Lisowski and R. L. Walter, unpublished; P. W. Lisowski, Ph.D. dissertation, Duke University, 1973 (unpublished).

¹⁰Th. Stammbach and R. L. Walter, Nucl. Phys. **A18**, 225 (1972).

$(\alpha, {}^2\text{He})$ Reaction as a Spectroscopic Tool for Investigating High-Spin States*

R. Jahn,† G. J. Wozniak, D. P. Stahel, and Joseph Cerny

Department of Chemistry and Lawrence Berkeley Laboratory, University of California, Berkeley, California 94720

(Received 28 June 1976)

A ${}^2\text{He}$ detection system has been developed and used to investigate the $(\alpha, {}^2\text{He})$ reaction at 65 MeV on ${}^{12}\text{C}$, ${}^{13}\text{C}$, and ${}^{16}\text{O}$ targets. Extreme spectroscopic selectivity with preferential population of final states with $(d_{5/2})^2_4^+$ character was observed. Applications of this experimental technique to the detection of other unbound reaction products are proposed.

Experimental systems capable of detecting nuclear reaction products in resonant final states with good efficiency and energy resolution can open up a wide range of unexplored nuclear reactions. Although at present such studies are largely confined to the detection of ${}^8\text{Be}$ nuclei,^{1,2} Robson³ has pointed out many other interesting resonant systems which can be detected as reaction products. Additionally, the well known final-state interaction in the two-nucleon 1S_0 , $T = 1$ system can be utilized; in particular, this interac-

tion in the ${}^2\text{He}$ system localizes the two breakup protons into a narrow cone. Thus ${}^2\text{He}$ can readily be detected with two proton detectors arranged in an appropriate geometry, and a few results on single neutron transfer via the $({}^3\text{He}, {}^2\text{He})$ reaction have been reported.^{4,5}

A very interesting reaction which can be studied at reasonably high bombarding energies with such a detection system is $(\alpha, {}^2\text{He})$, potentially a direct $2n$ transfer reaction very similar to the direct $n\bar{p}$ -transfer reaction (α, d) . The demonstrat-

ed selectivity of the (α, d) reaction⁶⁻⁸ makes it a valuable spectroscopic tool with which to investigate high-spin states in nuclei with $T_z = T_z(\text{target})$, and therefore one can anticipate that the $(\alpha, {}^2\text{He})$ reaction might selectively populate high spin states in nuclei with $T_z = T_z(\text{target}) + 1$. This reaction is particularly appealing, since because of the unavailability of high-energy triton beams, the analogous (t, p) reaction has not been investigated under conditions which favor large angular momentum transfer—nor have more than a few $2n$ transfer reactions induced by heavy ions been reported (cf. Anyas-Weiss *et al.*⁹). We report here the results of this initial observation of the $(\alpha, {}^2\text{He})$ reaction on ${}^{12}\text{C}$, ${}^{13}\text{C}$, and ${}^{16}\text{O}$ targets induced by 65-MeV α particles from the Lawrence Berkeley Laboratory 88-in. cyclotron. These data indicate the expected high selectivity of this reaction and its usefulness as an important spectroscopic tool.

Although detection of the two protons from in-flight breakup of ${}^2\text{He}$ is similar to detecting ${}^8\text{Be}$ decay via its two α particles, a difference arises in that the disintegration energy of ${}^2\text{He}$ does not originate from the breakup of a narrow state as is the case for ${}^8\text{Be}$, but is rather a distribution described by the Watson-Migdal formalism.¹⁰ In the following discussion of the ${}^2\text{He}$ detector, we assumed for simplicity that the breakup energy of the ${}^2\text{He}$ system was given by the "average" value of this distribution (400 keV).

The two protons arising from the breakup of ${}^2\text{He}$ are emitted into a cone in the laboratory, which is defined by the center-of-mass energy of the ${}^2\text{He}$ system and by its breakup energy. In order to achieve good detection efficiency, the acceptance angle of the two coincident proton telescopes has to be similar to the size of the breakup cone, which is approximately 15° for 40-MeV ${}^2\text{He}$ events. On the other hand, energy resolution considerations require a small angular acceptance to minimize kinematic broadening. An excellent compromise between efficiency and energy resolution is obtained by arranging the two proton telescopes vertically, thus achieving relatively good efficiency as a result of the large vertical acceptance angle, and reasonably good energy resolution by limiting the horizontal acceptance angle.

Figure 1(a) shows the ${}^2\text{He}$ detection system, consisting of two ΔE - E counter telescopes. The ΔE detectors were phosphorus-diffused Si, 380 μm thick, and the E detectors were Si(Li), 5 mm thick, all having the same area of $1 \times 1.4 \text{ cm}^2$.

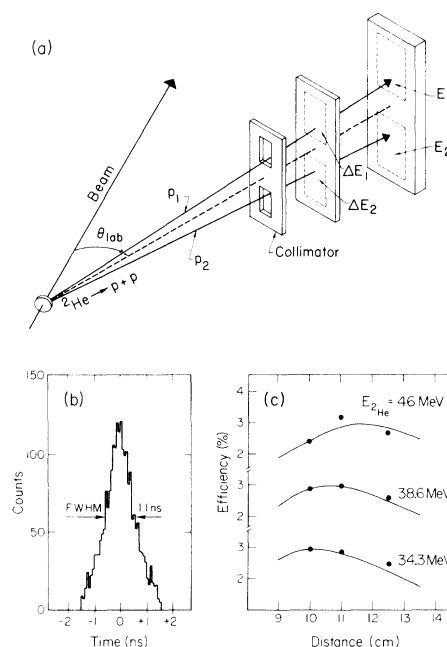


FIG. 1. (a) Schematic diagram of the ${}^2\text{He}$ detection system. (b) Spectrum of the time-of-flight difference between the two breakup protons. (c) Comparison of experimental (dots) and theoretical (solid lines) ${}^2\text{He}$ detection efficiencies as a function of the distance between target and collimator. The experimental efficiencies have been normalized to the calculations at a distance of 10 cm; errors lie within data points.

Two collimator slits separated by a post were employed, so that the system subtended a 15° vertical and a 4° horizontal acceptance angle. The ${}^2\text{He}$ events were identified by using standard particle identification techniques as well as subnanosecond fast timing between the two ΔE counters, which drastically reduced random events. In addition, fast pileup rejection was utilized so that high singles counting rates (30 kHz) could be tolerated in the ΔE counters.

Figure 1(b) shows the relative time distribution of observed proton coincidences from the reaction ${}^{13}\text{C}(\alpha, {}^2\text{He}){}^{15}\text{C}$ at 13° lab angle. The observed full width at half-maximum (FWHM) (1.1 nsec) of the distribution of flight time differences for the two protons agrees with predictions based on the assumption of 400-keV breakup energy (random coincidences from a single beam burst would have spanned up to 12 nsec FWHM). The coincidence counting rate was measured at different geometries obtained by varying the distance between the target and the collimator. Figure 1(c) depicts the relative experimental efficiency versus the calculated efficiency^{1,11} for three differ-

ent ${}^2\text{He}$ energies at three distances. The experimental data, normalized at 10 cm, are well reproduced by the calculations. The agreement between the calculated and experimental relative efficiencies and the narrow peak in the distribution of flight time differences require that the majority of the detected pp coincidences come from the breakup of the unbound ${}^2\text{He}$ system.

Representative spectra from the $(\alpha, {}^2\text{He})$ reaction on ${}^{12}\text{C}$, ${}^{13}\text{C}$ (90% enriched), and ${}^{16}\text{O}$ (as SiO_2) at forward angles are presented in Fig. 2. The experimental energy resolution of 350 keV was principally determined by kinematic broadening due to the 4° acceptance angle. As can be seen in the spectra, the $(\alpha, {}^2\text{He})$ reaction is extremely selective; only very few states in the residual nuclei are populated. In ${}^{14}\text{C}$ strong transitions were observed to a 3^- level at 6.73 MeV and to a 4^+ level at 10.55 MeV with weaker transitions to the ground state and to a level at 14.67 MeV. The ${}^{15}\text{C}$ spectrum shows only strong transitions to the $\frac{5}{2}^+$ level at 0.74 MeV and to two states at 6.85 and 7.35 MeV excitation energy, while in ${}^{18}\text{O}$ only population of the 4^+ level at 3.55 MeV was observed (weak transitions would be obscured because of the reactions on the Si in the target). It should be noted that these results on the ${}^{12}\text{C}$ and ${}^{16}\text{O}$ tar-

gets are similar to heavy-ion two-neutron transfer data⁹ and that in particular the 4^+ , 10.55-MeV state in ${}^{14}\text{C}$ was originally assigned via ${}^{12}\text{C}({}^{12}\text{C}, {}^{10}\text{C}){}^{14}\text{C}$ studies.⁹

Preferential population of high-spin states has been observed in the (α, d) reaction induced by 40–53-MeV α particles on many light nuclei^{6–8}; the selectively populated levels [e.g., of $(d_{5/2}^2)_{5^+}$ or $(f_{7/2}^2)_{7^+}$ character] correspond to particular kinematically favored transitions in which the np pair can be simply captured in a relative triplet state about an undisturbed target core. Since similar kinematic behavior and Q values occur in the $(\alpha, {}^2\text{He})$ reaction, one also expects to observe predominantly high-spin states, but now those in which the nm pair is captured in a relative singlet state. At 65-MeV bombarding energy, the transferred angular momentum in a surface interaction on these targets is about $(4-5)\hbar$ and thus transitions to levels formed by capturing the two stripped neutrons into d orbitals with configurations of $(d_{5/2}^2)_{4^+}$ should be enhanced.⁶ The observed strong population of the 4^+ states in ${}^{14}\text{C}$ (at 10.55 MeV) and in ${}^{18}\text{O}$ (at 3.55 MeV), which have substantial $(d_{5/2}^2)_{4^+}$ character,^{12–14} is in agreement with this simple picture. Equally dominant transitions to states with possible configurations involving f orbitals such as $(d_{5/2}f_{7/2})_{5^-}$ or $(f_{7/2}^2)_{6^+}$ are expected and appear in reactions on targets in the $2s-1d$ shell¹¹ but will not be discussed here.

With regard to Fig. 2(a), except for the weak population of the ${}^{14}\text{C}$ ground state, transitions to the other observed states in ${}^{14}\text{C}$ can be explained as kinematically favored transitions to $S=0$ components in the known 6.73-MeV $(d_{5/2}p_{1/2})_{3^-}$ state¹² and in the 14.67-MeV state [possibly 4^+ ⁹ of $(d_{5/2}d_{3/2})_{4^+}$ character¹² though without additional calculations $(d_{5/2}f_{7/2})_{5^-}$ cannot be excluded].¹⁵

Figure 3 shows angular distributions of the ${}^{12}\text{C}(\alpha, {}^2\text{He}){}^{14}\text{C}$ transitions. As in the (α, d) results,^{6,7} transitions to all the strongly populated levels show angular distributions which are relatively structureless and forward peaked; also, as before, the weaker transitions (here to the ${}^{14}\text{C}$ ground state) show oscillatory behavior. The overall cross section is ~ 100 times smaller than that observed in the (α, d) reaction, which is comparable to the difference observed between nm and np transfer in heavy-ion reactions⁹—though not necessarily of the same origin.¹¹

Since the ${}^{12}\text{C}$ and ${}^{13}\text{C}$ targets only differ by a $p_{1/2}$ neutron, one expects the $(\alpha, {}^2\text{He})$ reaction on ${}^{13}\text{C}$ to populate preferentially the same two-neu-

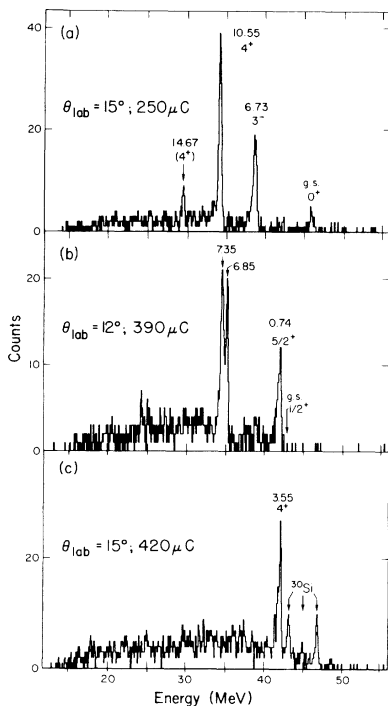


FIG. 2. ${}^2\text{He}$ energy spectra obtained from the reactions (a) ${}^{12}\text{C}(\alpha, {}^2\text{He}){}^{14}\text{C}$, (b) ${}^{13}\text{C}(\alpha, {}^2\text{He}){}^{15}\text{C}$, and (c) ${}^{16}\text{O}(\alpha, {}^2\text{He}){}^{18}\text{O}$ at an α -particle energy of 65 MeV.

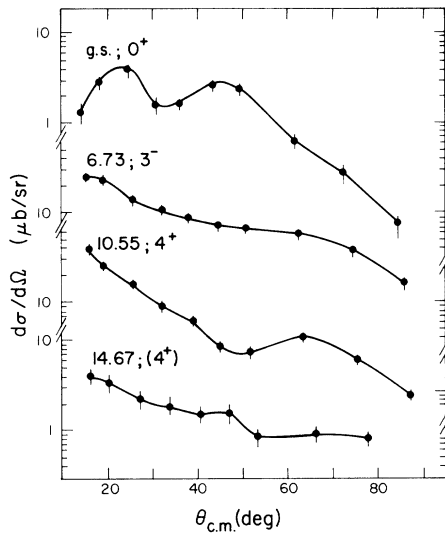


FIG. 3. Absolute differential cross sections for the reaction $^{12}\text{C}(\alpha, {}^2\text{He})^{14}\text{C}$ at 65 MeV. Statistical error bars are shown. The solid curves are meant to guide the eye.

tron configurations originally observed in reactions on ^{12}C , but now coupled to the $\frac{1}{2}^-$ target core. Thus the states observed in the ^{14}C spectrum should be split into two components in the ^{15}C spectrum, as has been observed in the analogous (α, d) reactions on ^{12}C and ^{13}C . Noting Fig. 2(b), then the doublet observed at 6.85–7.35 MeV in ^{15}C can be interpreted as having a configuration $[\{^{12}\text{C}(0^+)p_{1/2}\}_{1/2^-} \otimes (d_{5/2}^2)_{4^+}]_{7/2^-, 9/2^-}$. Although this model does not predict the assignment of spins to the two components of the split state, relative enhancement via the $(2J+1)$ statistical factor implies that the 7.35-MeV level might have the higher spin ($\frac{9}{2}^-$) because of its larger cross section. States at these excitation energies in ^{15}C have been observed in other reactions,¹⁶ but definite spin assignments have not been reported. Since the $\frac{5}{2}^+$ state at 0.74 MeV has a configuration $[\{^{12}\text{C}(0^+)p_{1/2}\}_{1/2^-} \otimes p_{1/2}d_{5/2}]_{5/2^+}$, the $p_{1/2}$ neutron of ^{13}C and the transferred $p_{1/2}$ neutron must couple to spin 0 and no splitting can arise. These three $^{13}\text{C}(\alpha, {}^2\text{He})^{15}\text{C}$ transitions and the $^{16}\text{O}(\alpha, {}^2\text{He})^{18}\text{O}$ transition to the 3.55-MeV $(d_{5/2}^2)_{4^+}$ state all show forward-peaked, structureless angular distributions. In addition, the observed cross sections of the transitions to the known 4^+ state in ^{14}C (10.55 MeV), to the sum of the split states in ^{15}C , and to the 4^+ state in ^{18}O are all equal within errors, which is further evidence for the assumption of a common $(d_{5/2}^2)_{4^+}$ configuration for these states.

These results clearly demonstrate the utility of

the $(\alpha, {}^2\text{He})$ reaction as a new spectroscopic tool capable of locating many unobserved two-neutron states of high spin in the $2s-1d$ and higher shells. Furthermore, extension of this approach toward studying resonant final systems as reaction products to other cases seems particularly practical and fruitful. As will be reported elsewhere,¹⁷ the present ${}^2\text{He}$ detection system simultaneously observes (at comparable yields) transitions of the α particle to its 0^+ first excited state (α^*) at 20.1 MeV (observed via its $p+t$ decay products). In addition, though only observed in low yield with this system, the study of transitions to the 16.7-MeV excited state of ${}^5\text{He}$ (${}^5\text{He}^* \rightarrow d+t$) would be readily permitted with minor geometric modifications. As one example, future studies of single- and two-neutron pickup via such unusual spectroscopic probes as $({}^3\text{He}, \alpha^*)$ and $({}^3\text{He}, {}^5\text{He}^*)$, respectively, might provide new insights into our knowledge of nuclear reaction mechanisms.

We would like to thank J. Walton for fabricating the large-area detectors.

*Work performed under the auspices of the U. S. Energy Research and Development Administration.

†On leave from Institut für Strahlen- und Kernphysik der Universität Bonn, Germany. Supported by Deutscher Akademischer Austauschdienst.

¹G. J. Wozniak, N. A. Jelley, and J. Cerny, Nucl. Instrum. Methods **120**, 29 (1974).

²J. L. Artz, M. B. Greenfield, and N. R. Fletcher, Phys. Rev. C **13**, 156 (1976).

³D. Robson, Nucl. Phys. **A204**, 523 (1973).

⁴R. van Dantzig *et al.*, Nucl. Instrum. Methods **92**, 205 (1971).

⁵D. M. Stupin, R. A. Ristinen, and P. Schwandt, Nucl. Phys. **A173**, 286 (1971).

⁶E. Rivet, R. H. Pehl, J. Cerny, and B. G. Harvey, Phys. Rev. **141**, 1021 (1966).

⁷C. C. Lu, M. S. Zisman, and B. G. Harvey, Phys. Rev. **186**, 1086 (1969).

⁸H. Nann, W. S. Chien, A. Saha, and B. H. Wildenthal, Phys. Lett. **60B**, 32 (1975).

⁹N. Anyas-Weiss, J. C. Cornell, P. S. Fisher, P. N. Hudson, A. Menchaca-Rocha, D. J. Millener, A. D. Panagiotou, D. K. Scott, D. Strottman, D. M. Brink, B. Buck, P. J. Ellis, and T. Engeland, Phys. Lett. **12C**, 201 (1974).

¹⁰J. C. Davis, J. D. Anderson, S. M. Grimes, and C. Wong, Phys. Rev. C **8**, 863 (1973), and references therein.

¹¹R. Jahn, D. P. Stahel, G. J. Wozniak, and J. Cerny, to be published.

¹²W. W. True, Phys. Rev. **130**, 1530 (1963).

¹³S. Lie, Nucl. Phys. **A181**, 517 (1972).

¹⁴T. T. S. Kuo and G. E. Brown, Nucl. Phys. **85**, 40

(1966).

¹⁵It should be noted that configurations containing a nucleon in the $d_{3/2}$ shell are apparently not preferentially populated in (α, d) reactions (see Ref. 6).

¹⁶J. D. Garrett, F. Ajzenberg-Selove, and H. G. Bingham, Phys. Rev. C **10**, 1730 (1974).

¹⁷R. Jahn, D. P. Stahel, G. J. Wozniak, J. Cerny, and H. P. Morsch, to be published.

Observation of a Low-Energy Octupole Resonance in Medium-Mass Nuclei*

J. M. Moss, D. H. Youngblood, C. M. Rozsa, D. R. Brown, and J. D. Bronson
Cyclotron Institute and Physics Department, Texas A&M University, College Station, Texas 77843
 (Received 7 July 1976)

A giant-resonance-like structure at $E_{exc} \sim 32/A^{1/3}$ MeV is observed in (α, α') spectra in nuclei from ^{90}Zr to ^{154}Sm . Analysis of the angular distributions leads to an assignment of $J^\pi = 3^-$ and an energy-weighted sum-rule fraction of 16–22% for this structure. Comparison with random-phase-approximation calculations shows that $\sim \frac{2}{3}$ of the expected $1\hbar\omega$ octupole energy-weighted sum-rule strength is found at $\sim 32/A^{1/3}$ MeV; the remainder occurs in low-lying 3^- states.

The giant dipole resonance and the more recently discovered giant quadrupole resonance are excellent examples of collective modes of motion whose properties are strongly influenced by nuclear shell structure. The excitation energies and large energy-weighted sum-rule (EWSR) strengths of these resonances are understandable in terms of a schematic model,^{1,2} which has as its basis the harmonic oscillator shell model. The harmonic oscillator model may also be used as a guide for vibrational modes of higher multipolarity.² In particular, for $L=3$ there are two fundamental modes, i.e., degenerate groups of states, at excitation energies of $1\hbar\omega$ and $3\hbar\omega$ which carry 25% and 75%, respectively, of the octupole EWSR strength. Coupling of these modes with an octupole-octupole (O-O) residual interaction results in two "giant resonances" which we term low-energy and high-energy octupole resonances (LEOR and HEOR) that exhaust $\sim 35\%$ and $\sim 65\%$, respectively, of the octupole EWSR (the exact partitioning depends on the strength of the coupling). Whether or not real nuclei generally exhibit such octupole giant-resonance-like structures is not known. The existence of a very collective low-energy 3^- state has been known for many years. However, with exceptions in the Pb isotopes, only a few percent (generally less than 10%) of the EWSR is accounted for by these states. Recent electron scattering data³ indicate that a large portion of the missing $E3$ strength is between 5 and 10 MeV in ^{116}Sn . We present here evidence from the inelastic scattering of 96- and 115-MeV α particles that the isoscalar octupole EWSR strength in nuclei between $A=90$ and $A=154$ exhibits a giant-resonance-like structure in a broad state

(or group of states) at $\sim 32/A^{1/3}$ MeV. The EWSR strength observed in this region is from $\frac{1}{2}$ to $\frac{2}{3}$ of that expected for the lower state predicted by the schematic model; thus we will refer to the structure at $32/A^{1/3}$ MeV as the LEOR. Combination of the octupole EWSR observed in the LEOR plus that from low-lying 3^- states accounts for essentially all of the oscillator strength expected to lie at $E_x \lesssim 1\hbar\omega$ in these nuclei.

The experimental apparatus and procedure used has been thoroughly described in a recent publication.⁴ Spectra from the (α, α') reaction near expected maxima for $L=3$ are shown in Fig. 1 for several targets. Also shown for comparison is a portion of the spectrum of ^{148}Sm at a minimum angle for $L=3$, maximum for $L=2$. Energy resolution varied from 150 keV at forward angles to 240 keV at backward angles. Analysis of the broad group of states at $\sim 32/A^{1/3}$ MeV was accomplished in the following manner. First, impurity peaks due to ^{16}O and ^{12}C were fitted with Gaussian peak shapes and subtracted from the spectra. A multiple-peak fit consisting of a superposition of narrow (~ 200 keV) and broad (1–2 MeV) Gaussians plus background was then applied to the spectra. Backgrounds were chosen by drawing a line from the minimum just above the broad peak to one just below. The angular distribution of the subtracted background showed a monotonic decrease with increasing angle. In ^{90}Zr and ^{142}Nd , states of multipolarity different from 3^- were recognized by their angular distribution and are indicated by shading in Fig. 1. Octupole strength in ^{90}Zr was found in a multiplet consisting of at least six levels plus high-energy tail which was not resolved into separate peaks.